

Electronic Supplementary Information (ESI)

Design, synthesis and *in-silico* screening of Benzoxazole-Thiazolidinone hybrids as potential inhibitors of SARS-CoV-2 proteases

Cheerala Vijay Sai Krishna^a, Prasanth Ghanta^b, C N Sundaresan^{a*}

^a *Department of Chemistry, Brindavan Campus, Sri Sathya Sai Institute of Higher Learning, Bangalore 560067, India*

^b *Department of Biosciences, Prasanthi Nilayam Campus, Sri Sathya Sai Institute of Higher Learning, Puttaparthi 515134, India*

SD-1: Similarity Study using Osiris Datawarrior

* Corresponding author. Email: cnsundaresan@sssihl.edu.in

A similarity study comparing the B-T hybrids and 315 compounds tested for their effectiveness as inhibitors of SARS-CoV-2 retrieved from ChEMBL (Target ID: ChEMBL4303835) was carried out using Osiris DataWarrior. The results of this study indicated that a few of the hybrids shared a similarity of approximately 0.6 (Tables 1 & 2) with the screened molecules.

Table 1 Similarity of BT series with the tested compounds against SARS-CoV-2

S. No.	B-T hybrids	Screened molecules	Similarity (SkelSpheres)
1	BT9	ChEMBL1459140	0.61
2	BT3	ChEMBL374632	0.60
3	BT4	ChEMBL374632	0.61
4	BT6	ChEMBL374632	0.61
5	BT7	ChEMBL27289	0.62
		ChEMBL374632	0.61
		ChEMBL565269	0.60
6	BT8	ChEMBL374632	0.62
7	BT10	ChEMBL374632	0.61
		ChEMBL565269	0.60
8	BT11	ChEMBL374632	0.62
		ChEMBL152649	0.62
		ChEMBL27289	0.60
9	BT12	ChEMBL374632	0.62
10	BT14	ChEMBL374632	0.61
11	BT25	ChEMBL374632	0.62
12	BT26	ChEMBL540612	0.61
		ChEMBL208943	0.61
		ChEMBL3746912	0.61
13	BT17	ChEMBL374632	0.63
14	BT23	ChEMBL4303151	0.61
15	BT18	ChEMBL374632	0.62
17	BT15	ChEMBL374632	0.64
18	BT16	ChEMBL1671971	0.60

Table 2 Similarity of CBT series and MBT series with the tested compounds against SARS-CoV-2

S. No.	B-T hybrids	Screened molecules	Similarity (SkelSpheres)
1	CBT4	CHEMBL27289	0.60
2	CBT26	CHEMBL75232	0.61
3		CHEMBL208943	0.61
4	CBT2	CHEMBL27289	0.60
		CHEMBL2106227	0.61
6	CBT25	CHEMBL4303404	0.62
7	CBT24	CHEMBL1230165	0.63
8	CBT16	CHEMBL1671971	0.61
9	CBT5	CHEMBL254578	0.62
10	CBT9	CHEMBL2363137	0.60
		CHEMBL1459140	0.61
11	CBT9	CHEMBL1448	0.63
12	CBT13	CHEMBL2363137	0.60
		CHEMBL1448	0.62
13	MBT26	CHEMBL208943	0.61
14	MBT5	CHEMBL254578	0.60
15	MBT9	CHEMBL1459140	0.61
16	MBT16	CHEMBL1671971	0.60

SD-2: Structure of PLp

The protein structure was directly taken from this particular study¹, after simulating it for 20ns. The structure has a sequence similarity of 98.4%, pocket similarity of 100% and structural similarity of 96.7% with the available crystal structure of papain-like protease of SARS-CoV-2 (PDB ID: 6W9C).

Table 3 Binding energies of BT series with 3CLP from the docking studies

BT Series	Binding Energy	BT Series	Binding Energy
BT1	-6.45	BT15	-7.93
BT2	-8.27	BT16	-6.77
BT3	-8.32	BT17	-6.44
BT4	-7.57	BT18	-7.66
BT5	-7.85	BT19	-7.83
BT6	-8.55	BT20	-7.46
BT7	-7.63	BT21	-7.91
BT8	-7.98	BT22	-8.08
BT9	-8.32	BT23	-7.83
BT10	-8.87	BT24	-7.81
BT11	-7.53	BT25	-7.79
BT12	-7.59	BT26	-8.3
BT13	-8.01	BT27	-7.54
BT14	-8.49		

Table 4 Binding energies of CBT series with 3CLp from the docking studies

CBT Series	Binding Energy	CBT Series	Binding Energy
CBT1	-7.74	CBT15	-8.23
CBT2	-7.17	CBT16	-6.74
CBT3	-7.32	CBT17	-6.23
CBT4	-8.33	CBT18	-7.32
CBT5	-6.95	CBT19	-8.32
CBT6	-7.59	CBT20	-7.92
CBT7	-7.51	CBT21	-8.28
CBT8	-7.69	CBT22	-8.49
CBT9	-7.58	CBT23	-8.72
CBT10	-7.71	CBT24	-7.32
CBT11	-6.85	CBT25	-7.13
CBT12	-6.42	CBT26	-8.31
CBT13	-6.82	CBT27	-6.63
CBT14	-7.44		

Table 5 Binding energies of MBT series with 3CLp from the docking studies

MBT Series	Binding Energy	MBT Series	Binding Energy
MBT1	-7.05	MBT15	-8.53
MBT2	-7.45	MBT16	-8.21
MBT3	-7.6	MBT17	-6.5
MBT4	-7.44	MBT18	-6.68
MBT5	-7.36	MBT19	-7.28
MBT6	-7.85	MBT20	-8.04
MBT7	-7.37	MBT21	-6.89
MBT8	-7.58	MBT22	-7.1
MBT9	-8.22	MBT23	-8.85
MBT10	-8.01	MBT24	-7.36
MBT11	-7.22	MBT25	-7.12
MBT12	-6.76	MBT26	-8.31
MBT13	-7.22	MBT27	-7.56
MBT14	-7.86		

Table 6 Binding energies of BT series with PLP from the docking studies

BT Series	Binding Energy	BT Series	Binding Energy
BT1	-5.43	BT15	-5.98
BT2	-6	BT16	-6.02
BT3	-6.06	BT17	-5.94
BT4	-6.16	BT18	-6.16
BT5	-6.79	BT19	-6.03
BT6	-6.49	BT20	-5.97
BT7	-6.11	BT21	-6.06
BT8	-6.21	BT22	-5.92
BT9	-7.66	BT23	-6
BT10	-6.43	BT24	-7.74
BT11	-6.42	BT25	-7.16
BT12	-6.5	BT26	-6.79
BT13	-6.87	BT27	-9.03
BT14	-6.15		

Table 7 Binding energies of CBT series with PLp from the docking studies

CBT Series	Binding Energy	CBT Series	Binding Energy
CBT1	-5.21	CBT15	-6.22
CBT2	-6.49	CBT16	-6.72
CBT3	-6.54	CBT17	-6.3
CBT4	-6.34	CBT18	-6.44
CBT5	-6.63	CBT19	-5.93
CBT6	-6.74	CBT20	-6.16
CBT7	-6.17	CBT21	-6.55
CBT8	-6.19	CBT22	-5.91
CBT9	-7.92	CBT23	-6.24
CBT10	-6.77	CBT24	-7.97
CBT11	-6.63	CBT25	-6.72
CBT12	-6.71	CBT26	-7.52
CBT13	-7.05	CBT27	-5.45
CBT14	-6.24		

Table 8 Binding energies of MBT series with PLp from the docking studies

MBT Series	Binding Energy	MBT Series	Binding Energy
MBT1	-5.36	MBT15	-6.26
MBT2	-6.47	MBT16	-6.33
MBT3	-6.56	MBT17	-6.32
MBT4	-6.31	MBT18	-6.77
MBT5	-6.62	MBT19	-6.16
MBT6	-6.72	MBT20	-6.29
MBT7	-6.66	MBT21	-5.98
MBT8	-6.47	MBT22	-6
MBT9	-7.96	MBT23	-6.34
MBT10	-6.75	MBT24	-7.91
MBT11	-6.61	MBT25	-6.63
MBT12	-6.67	MBT26	-7.58
MBT13	-7.03	MBT27	-6.68
MBT14	-6.26		

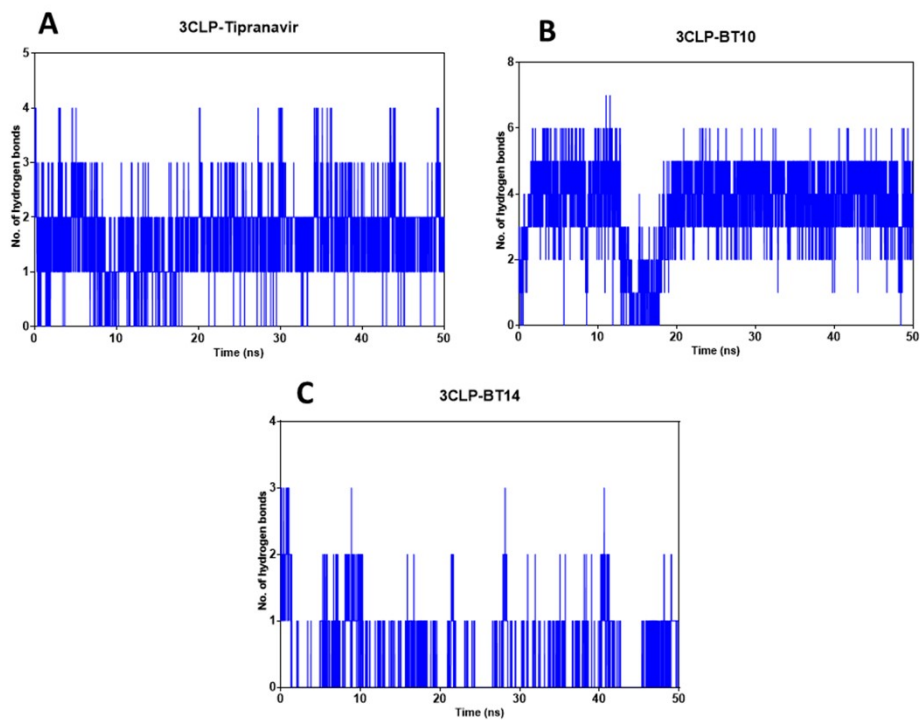


Fig. 1. Number of H-bonds throughout the trajectory of 3CLp-Tipranavir complex (A), 3CLp-BT10 complex (B) and 3CLp-BT14 complex (C)

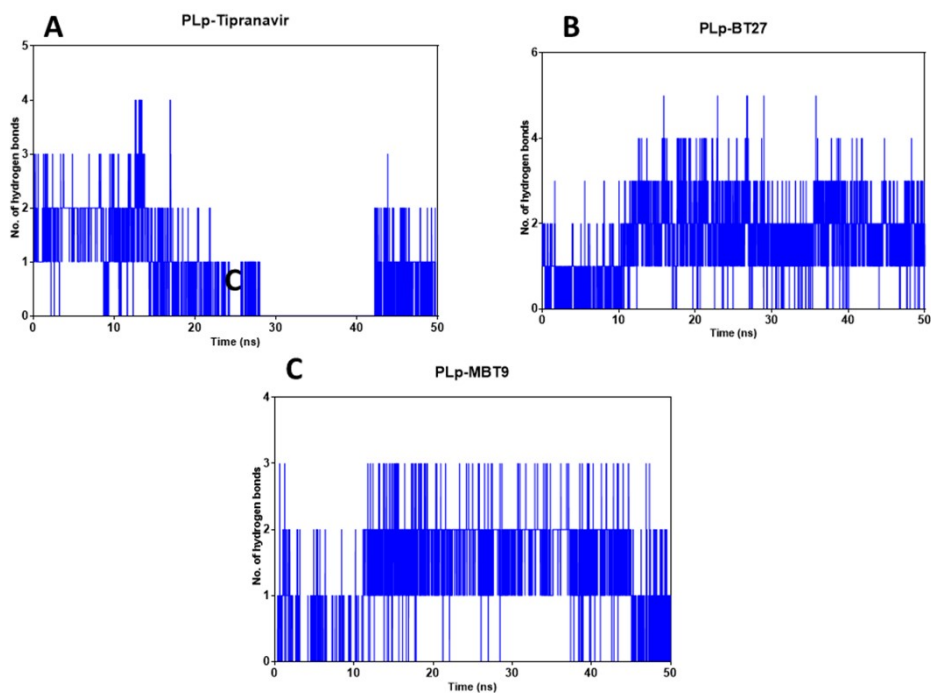


Fig. 2. Number of H-bonds throughout the trajectory of PLp-Tipranavir complex (A), 3CLp-BT27 complex (B) and 3CLp-MBT9 complex (C)

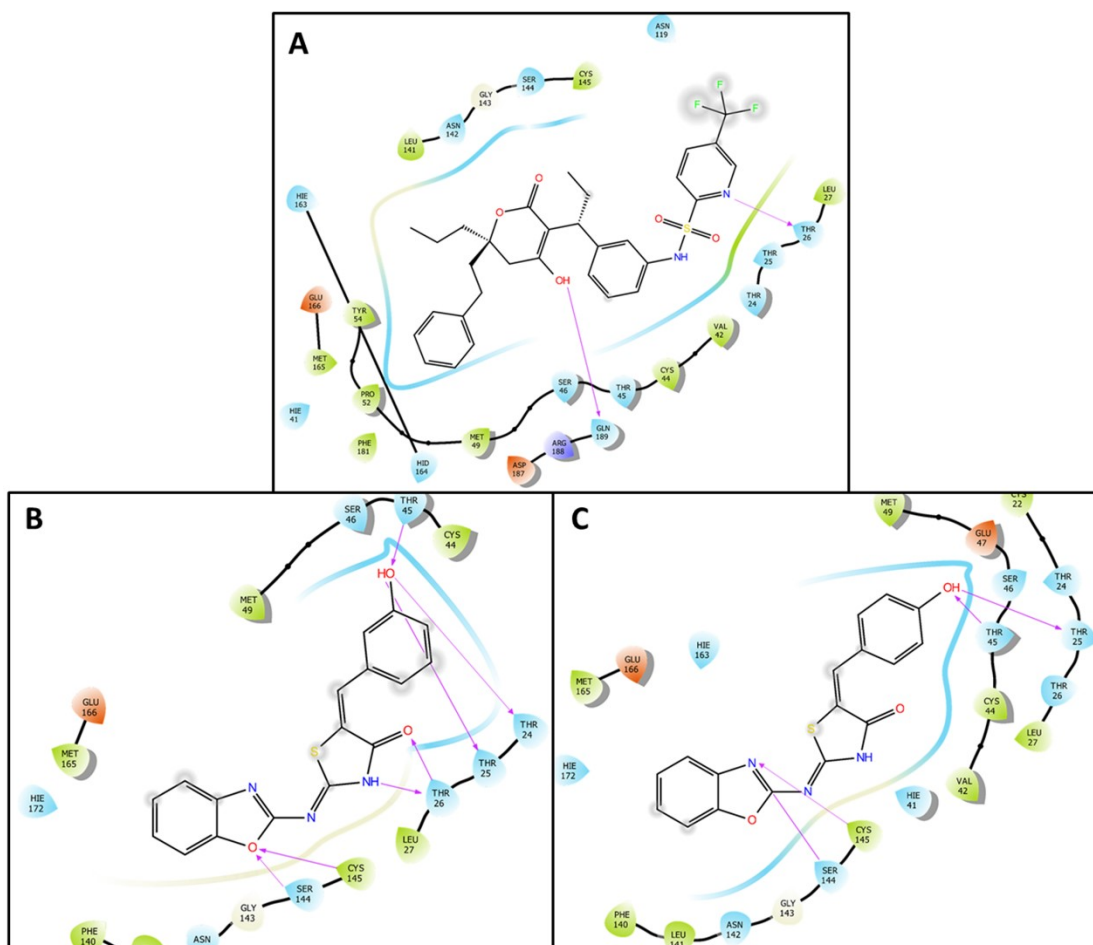


Fig. 3. Molecular interactions of Tipranavir (A), BT10 (B) and BT14 (C) with 3CLp from docking studies in 2D representation. The purple lines indicate the hydrogen bonding interactions, the red lines indicate pi-pi interactions, the green lines indicate pi-cation interactions of the ligands with active site residues.

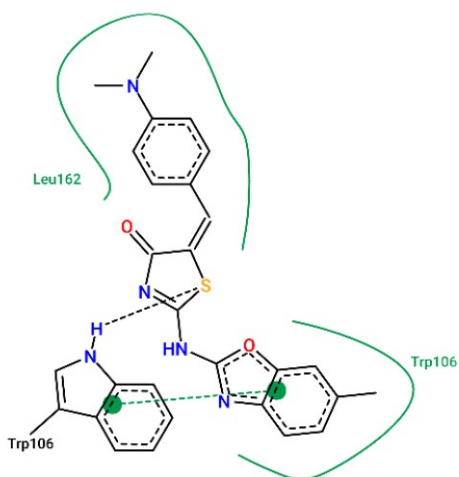


Fig. 4. Sulphur atom of MBT17 forming hydrogen bond with Trp106 of PLp.

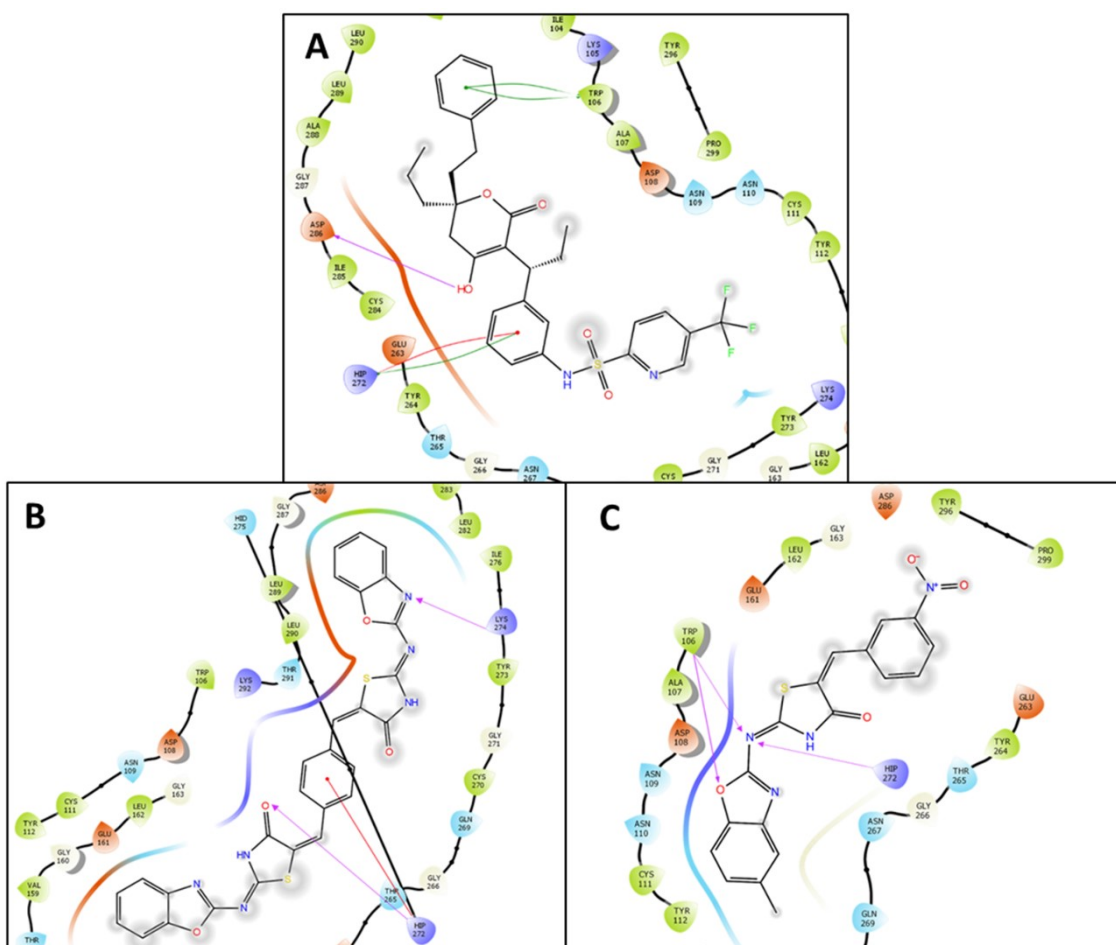


Fig. 5. Molecular interactions of Tipranavir (A), BT27 (B) and MBT9 (C) with 3CLp from docking studies in 2D representation. The purple lines indicate the hydrogen bonding interactions, the red lines indicate pi-pi interactions, the green lines indicate pi-cation interactions of the ligands with active site residues.

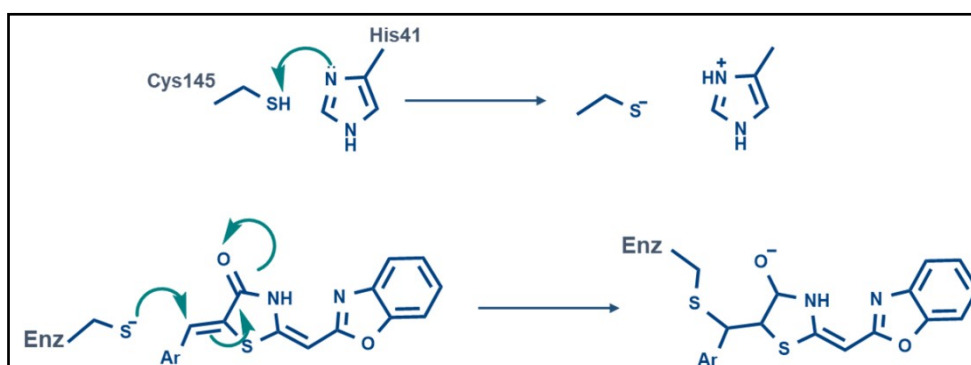
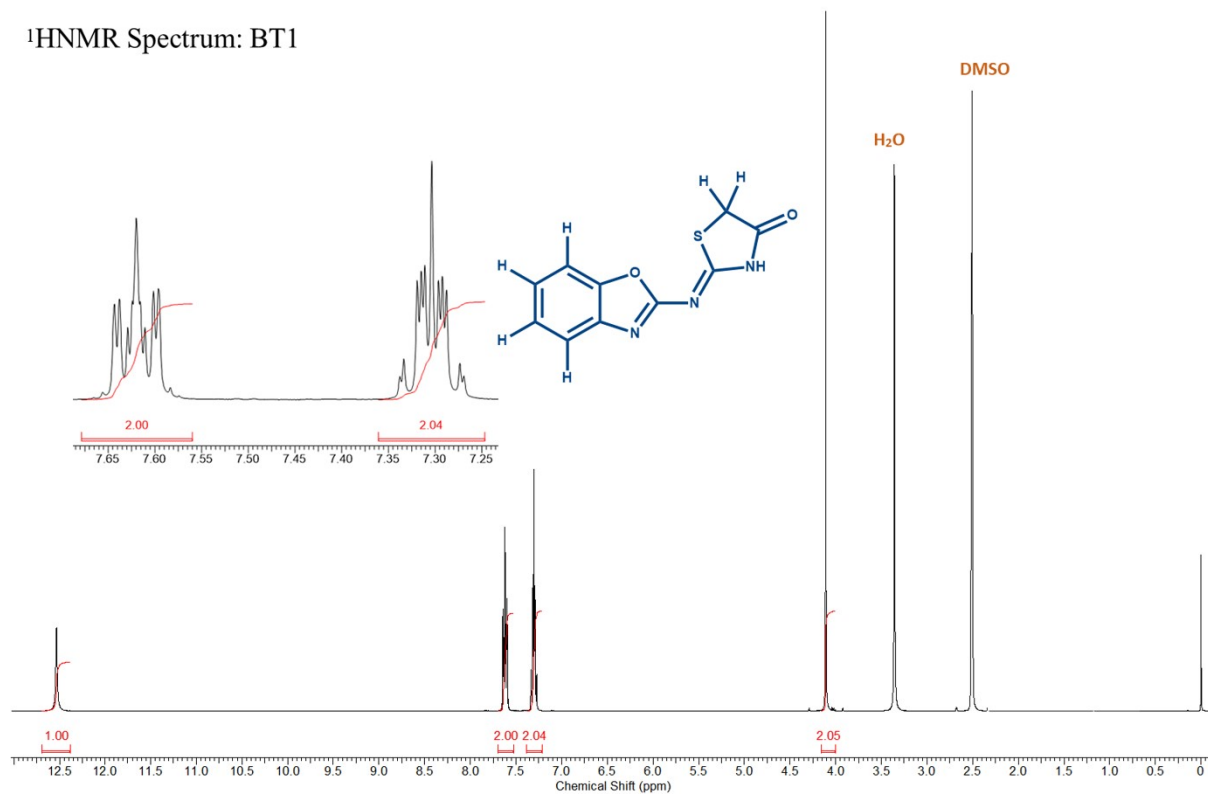
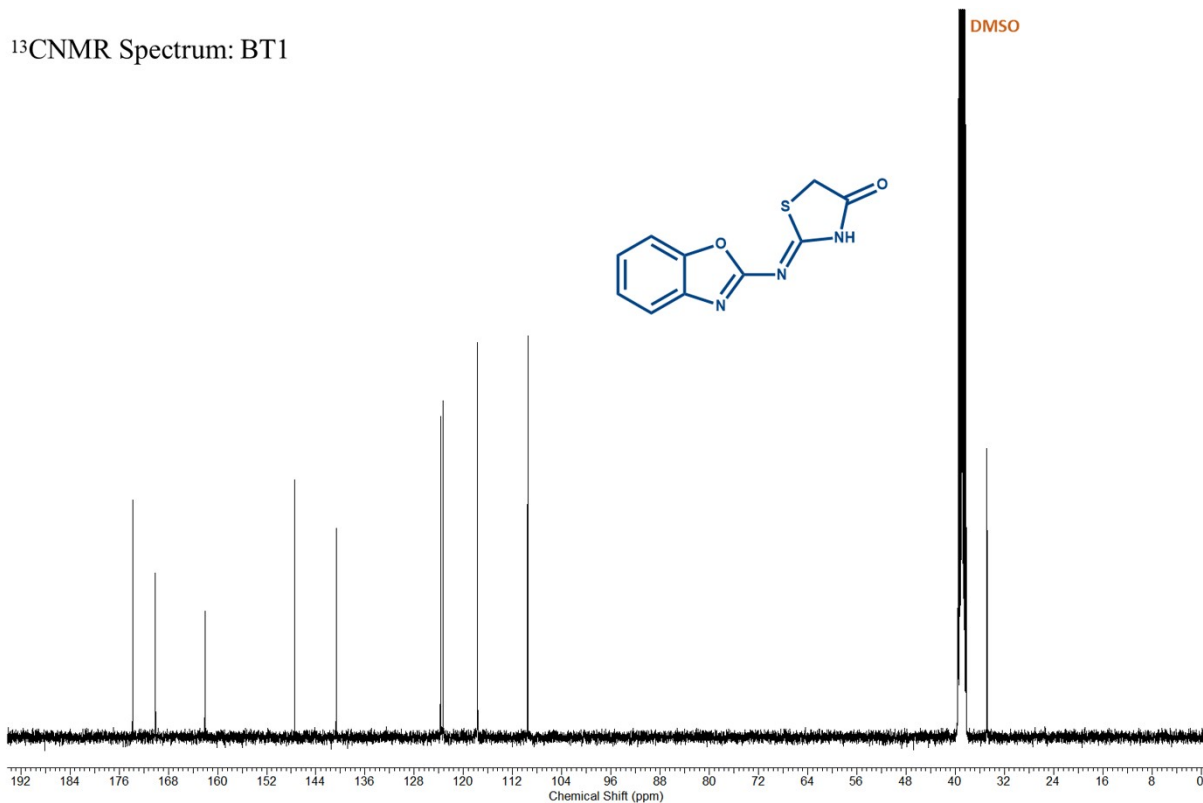


Fig. 6. Illustration of B-T hybrids as covalent binder to 3CLp of SARS-CoV-2. His41's imidazole group polarises and activates the Cys145's Thiol group, forming a highly nucleophilic Cys-S⁻ that would react with the Michael acceptor of α , β -unsaturated ketone group.

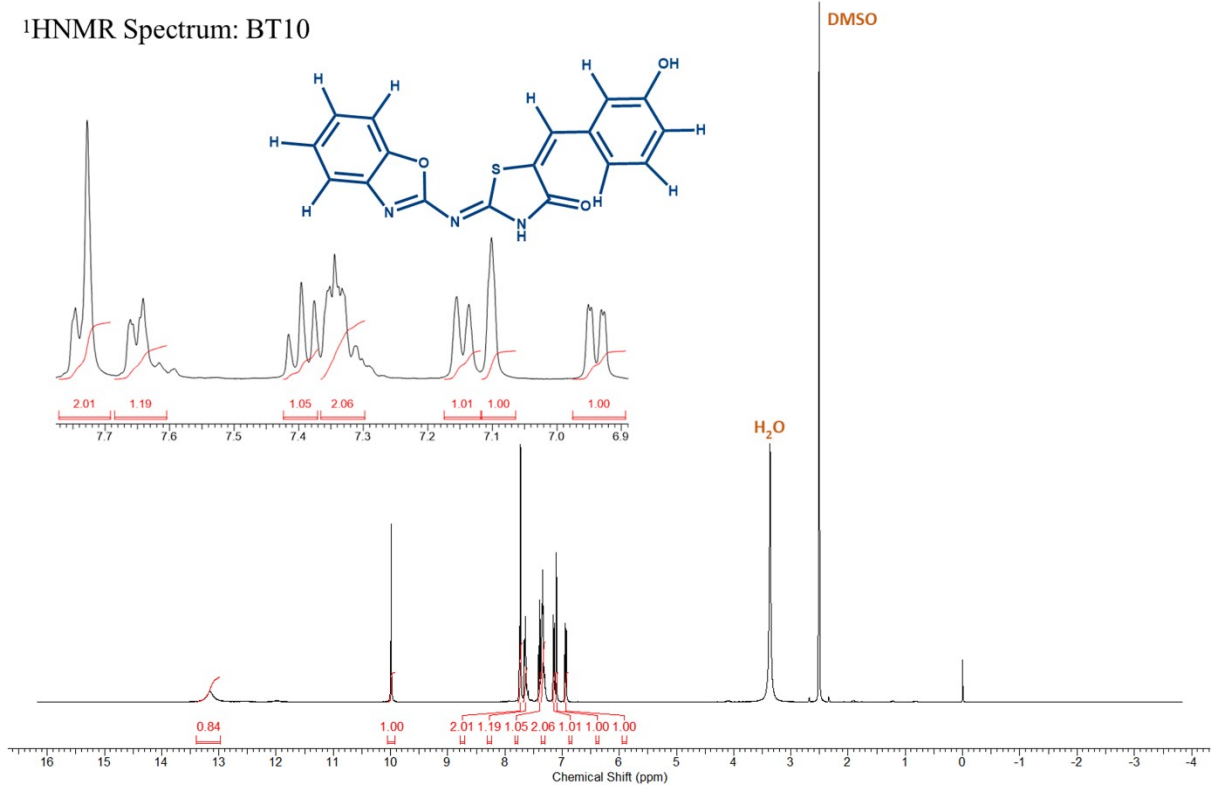
¹H NMR Spectrum: BT1



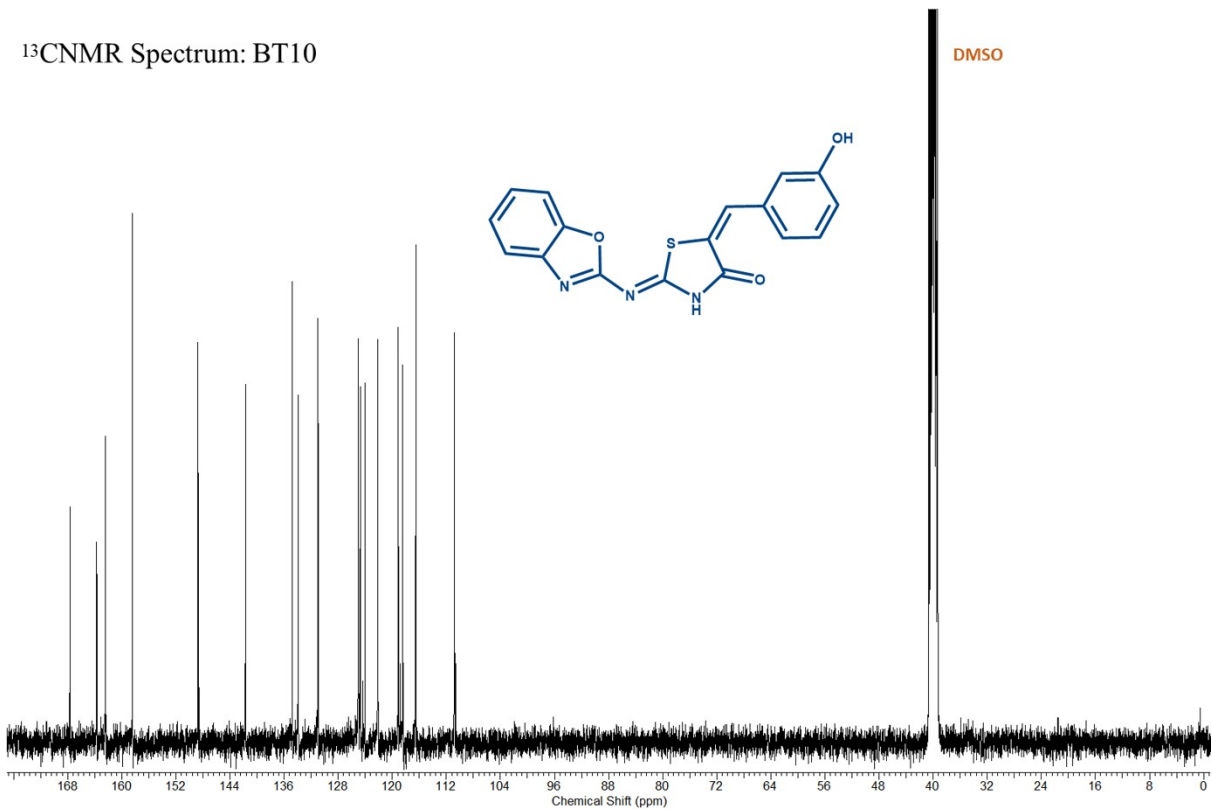
¹³C NMR Spectrum: BT1



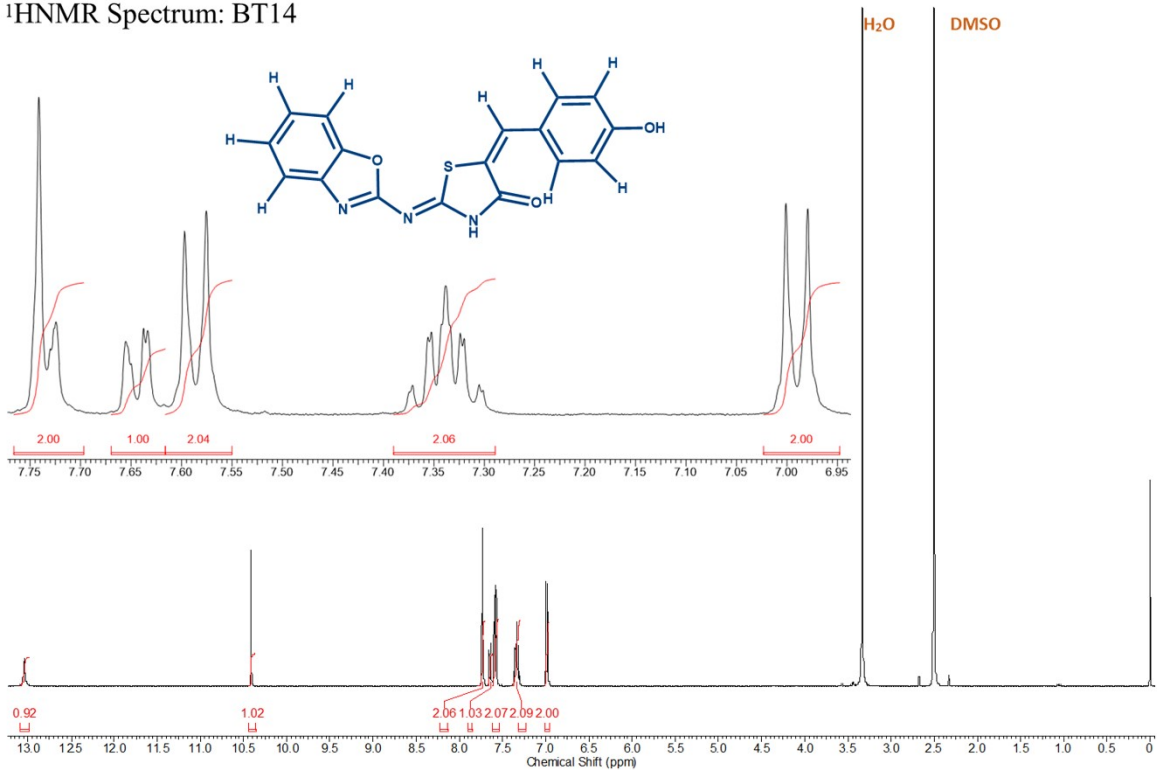
¹H NMR Spectrum: BT10



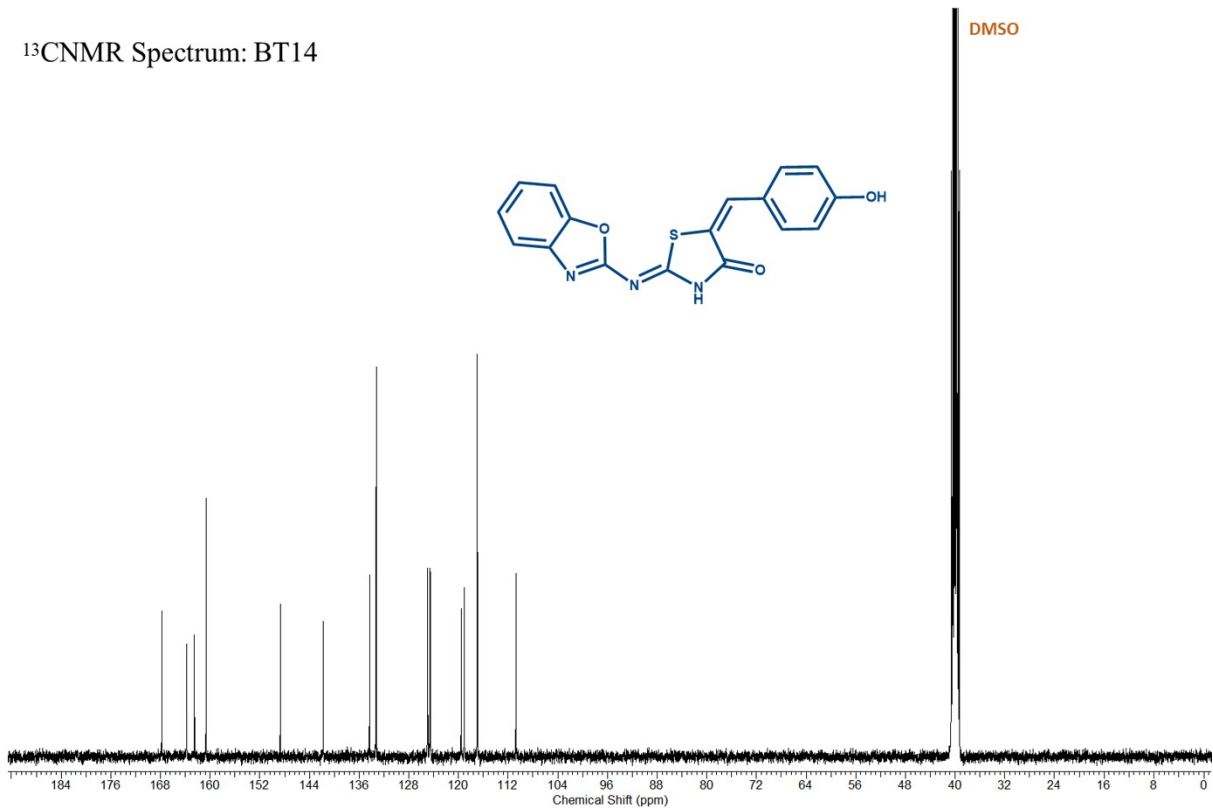
¹³C NMR Spectrum: BT10



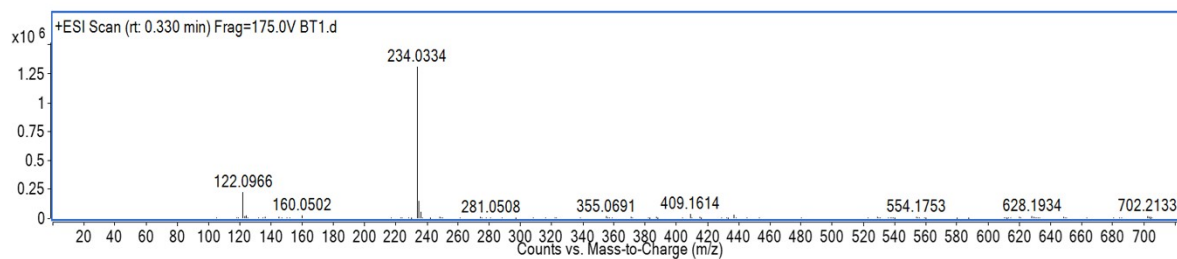
¹H NMR Spectrum: BT14



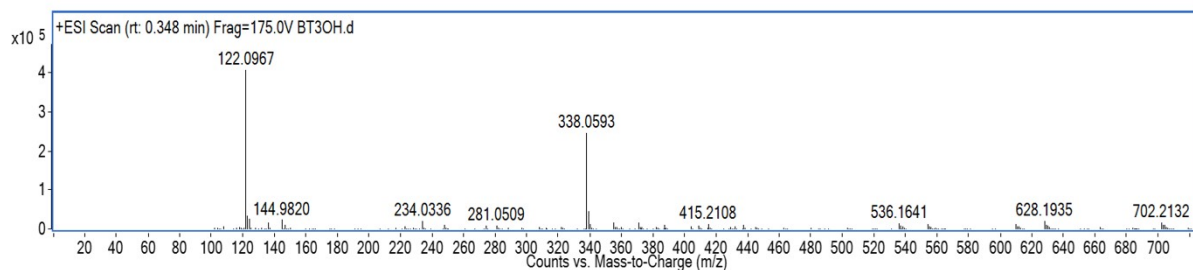
¹³C NMR Spectrum: BT14



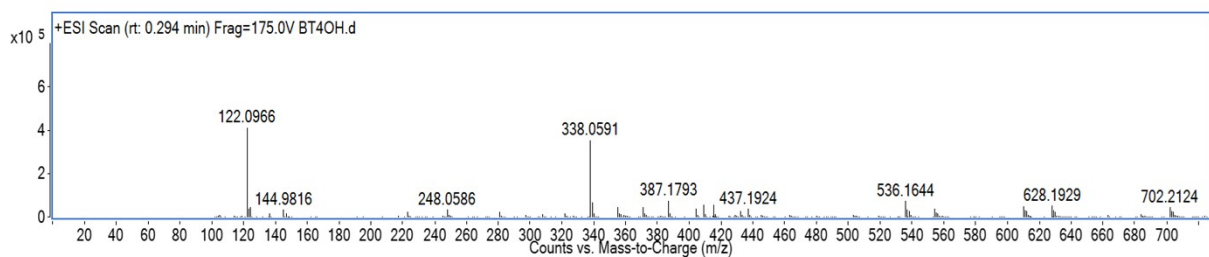
HRMS Profile: BT1



HRMS Profile: BT10



HRMS Profile: BT14



References

- 1 K. Mitra, P. Ghanta, S. Acharya, G. Chakrapani, B. Ramaiah and M. Doble, *J. Biomol. Struct. Dyn.*, 2020, **0**, 1–14.

